Selection of optimal artificial boundary condition (ABC) frequencies for structural damage identification

Selection of optimal artificial boundary condition (ABC) frequencies for structural damage identification

Lei Mao[1]*, Yong Lu[2]

[1] Department of Aeronautical and Automotive Engineering, Loughborough University, Epinal Way, Loughborough, LE11 3TU, UK

[2]School of Engineering, The University of Edinburgh, Faraday Building, The King's Buildings, Colin Maclaurin, Road, Edinburgh, ED9 3DW, UK

*Corresponding author: l.mao@lboro.ac.uk

Abstract

In this paper, the sensitivities of artificial boundary condition (ABC) frequencies to the damages are investigated, and the optimal sensors are selected to provide the reliable structural damage identification. The sensitivity expressions for one-pin and two-pin ABC frequencies, which are the natural frequencies from structures with one and two additional constraints to its original boundary condition, respectively, are proposed. Based on the expressions, the contributions of the underlying mode shapes in the ABC frequencies can be calculated and used to select more sensitive ABC frequencies. Selection criteria are then defined for different conditions, and their performance in structural damage identification is examined with numerical studies. From the findings, conclusions are given.

Key word: ABC frequency, structural damage identification, numerical simulation, sensitivity analysis, selection criteria

1. Introduction

Structural Health Monitoring (SHM) is an important subject in today's civil engineering practice. This is particularly true for large scale structures, for example, bridges and high-rise buildings, since severe damages or collapse of these structures will cause not only significant economic loss, but also loss of human lives. Therefore, the interest in the ability to monitor the structures and detect damage at an early stage becomes pervasive.

Among many other approaches to structural health monitoring and damage identification, model-based methods, in particular finite element model updating, have attracted extensive attention in the past few decades [1-13]. In such a procedure, the errors in a computational finite element model are corrected by minimizing the discrepancy between the measured and simulated response data. The parameters after updating may serve as indicators of the structural or damage conditions, while the updated FE model as a whole can be used for current and future performance predictions for the structure in question. The most commonly used response data for FE model updating are the dynamic modal data, such as natural frequencies, mode shapes, and to a lesser extent damping. However, in practical conditions, the noise contained in the response data, especially in mode shapes, dictate that only a limited amount of such data as acquired from a physical test may be useful in the actual FE model updating operation [14-16].

Comparing to the mode shapes, natural frequencies are generally known to be measurable with higher accuracy. However, natural frequencies are not sensitive to local damages. Moreover, since each natural mode has only one frequency, the total number of natural frequencies that can be measured with high quality is always limited [17-18]. These restrict the ability of using natural frequency alone in relatively complex problems involving a large number of variable parameters. It would be highly desirable if additional modal frequencies can be generated to enhance the frequency dataset in the general damage detection and structural identification field.

The concept of perturbed natural frequencies of a structure under different (perturbed) boundary conditions opens up a new avenue where more modal frequency data may be generated for damage identification [19-21]. The development of the theory of the artificial boundary condition (ABC) methodology, by which the above mentioned perturbed natural frequencies of the structure with additional pin supports could be derived from the incomplete FRF matrix measured from the original structure, as well as the subsequent studies on the effectiveness of such frequencies in structural identification, brings the incorporation of the perturbed natural frequencies a significant step closer to practical applications. Several researches have been devoted to the structural damage identification using ABC frequencies in the last few decades [22-27].

Despite the above advancements, since a large variety of perturbed boundary conditions, or the ABC pin supports, may be configured for the ABC frequencies, appropriate criteria for the selection of better (or more sensitive) ABC frequencies for inclusion in the structural identification or FE model updating need be developed.

In this paper, the sensitivities of ABC frequencies to the damages are investigated. For simplicity and without losing generality, only one-pin and two-pin ABC frequencies are employed. In the study, the approach of deriving anti-resonance (one-pin ABC frequencies) sensitivity expression for lightly damped structures is adopted and is extended to two-pin ABC frequencies. On the basis of the expressions of one-pin and two-pin ABC frequency sensitivities, the contributions of the underlying mode shapes in the ABC frequencies can be calculated, and this enables the selection of more sensitive ABC frequencies for FE model updating. Following the basic formulation, numerical studies are then used to examine the performance of the selected ABC frequencies in damage identification of a lightly damped structure. Moreover, the size of ABC frequencies for better identification performance is also studied. Finally, conclusions are given and future work is suggested.

2. Theory of ABC frequency sensitivities

2.1 Sensitivity of driving point anti-resonance (one-pin ABC frequencies) and mode shape contributions

In modal analysis, the frequency response function (FRF) of an un-damped system can generally be expressed as follows:

$$\mathbf{h}_{ij}(\omega) = \sum_{k=1}^{n} \frac{\boldsymbol{\varphi}_{ik}\boldsymbol{\varphi}_{jk}}{(\omega_k^2 - \omega^2)} \quad (1)$$

Where i,j represent positions of the excitation force and the response, respectively. $\boldsymbol{\varphi}_{\mathbf{ik}}$ and $\boldsymbol{\varphi}_{\mathbf{jk}}$ are the k-th order mode shape at points i and j, respectively, and $\omega_k$is the k-th order natural frequency.

When the applied force and measured response are at the same position, the corresponding FRF reduces to the driving-point FRF as:

$$\mathbf{h}_{ii}(\omega) = \sum_{k=1}^{n} \frac{\boldsymbol{\varphi}_{ik}^2}{(\omega_k^2 - \omega^2)} \tag{2}$$

According to Mottershead [28], Eq.(2) can be rearranged as follows:

$$\mathbf{h}_{ii}(\omega) = \sum_{k=1}^{n} \frac{\boldsymbol{\varphi}_{ik} det(\Lambda - \omega^2 I)_k \boldsymbol{\varphi}_{ik}}{\det(\Lambda - \omega^2 I)} \tag{3}$$

where $\det\left(\boldsymbol{\Lambda} - \omega^2 \mathbf{I}\right)_{\mathbf{k}} = \left(\omega_1^2 - \omega^2\right)\left(\omega_2^2 - \omega^2\right)\cdots\left(\omega_{k-1}^2 - \omega^2\right)\left(\omega_{k+1}^2 - \omega^2\right)\cdots\left(\omega_n^2 - \omega^2\right)$

The driving point anti-resonance frequencies, which are just one-pin ABC frequencies, can be obtained by setting Eq.(3) to zero, thus:

$$\sum_{k=1}^{n} \boldsymbol{\varphi}_{ik} det(\Lambda - \omega^2 I)_k \boldsymbol{\varphi}_{ik} = 0 \tag{4}$$

where ω_{1-pin_i} denotes anti-resonance from driving-point FRFs measured at point i (i.e. one-pin ABC frequency with pin at point i).

Differentiating each term in Eq. (4) with respect to a variable parameter p:

$$\begin{aligned}\frac{\partial}{\partial p}\left(\boldsymbol{\varphi}_{\mathbf{ik}} \det\left(\boldsymbol{\Lambda} - \omega_{1-pin\_i}^2 \mathbf{I}\right)_{\mathbf{k}} \boldsymbol{\varphi}_{\mathbf{ik}}\right) &= \frac{\partial \boldsymbol{\varphi}_{\mathbf{ik}}}{\partial p} \det\left(\boldsymbol{\Lambda} - \omega_{1-pin\_i}^2 \mathbf{I}\right)_{\mathbf{k}} \boldsymbol{\varphi}_{\mathbf{ik}} \\ &+ \boldsymbol{\varphi}_{\mathbf{ik}} \frac{\partial}{\partial p}\left(\det\left(\boldsymbol{\Lambda} - \omega_{1-pin\_i}^2 \mathbf{I}\right)_{\mathbf{k}}\right) \boldsymbol{\varphi}_{\mathbf{ik}} + \boldsymbol{\varphi}_{\mathbf{ik}} \det\left(\boldsymbol{\Lambda} - \omega_{1-pin\_i}^2 \mathbf{I}\right)_{\mathbf{k}} \frac{\partial \boldsymbol{\varphi}_{\mathbf{ik}}}{\partial p}\end{aligned} \tag{5}$$

Based on Mottershead [28] substituting Eq. (5) into Eq. (4) yields:

$$\frac{\partial \omega_{i-pin\_j}^2}{\partial p} = 2\times \frac{\sum_{k=1}^{n} \frac{\partial \boldsymbol{\varphi}_{\mathbf{ik}}}{\partial p} \det\left(\boldsymbol{\Lambda} - \omega_{i-pin\_j}^2 \mathbf{I}\right)_{\mathbf{k}} \boldsymbol{\varphi}_{\mathbf{ik}}}{\sum_{k=1}^{n} \boldsymbol{\varphi}_{\mathbf{ik}} \left(\sum_{\substack{p=1 \\ p\neq k}}^{n} \det\left(\boldsymbol{\Lambda} - \omega_{i-pin\_j}^2 \mathbf{I}\right)_{\mathbf{k,p}}\right) \boldsymbol{\varphi}_{\mathbf{ik}}} + \frac{\sum_{p=1}^{n} \frac{\partial \omega_p^2}{\partial p} \left(\sum_{\substack{k=1 \\ k\neq p}}^{n} \det\left(\boldsymbol{\Lambda} - \omega_{i-pin\_j}^2 \mathbf{I}\right)_{\mathbf{k,p}} \boldsymbol{\varphi}_{\mathbf{ik}} \boldsymbol{\varphi}_{\mathbf{ik}}\right)}{\sum_{k=1}^{n} \boldsymbol{\varphi}_{\mathbf{ik}} \left(\sum_{\substack{p=1 \\ p\neq k}}^{n} \det\left(\boldsymbol{\Lambda} - \omega_{i-pin\_j}^2 \mathbf{I}\right)_{\mathbf{k,p}}\right) \boldsymbol{\varphi}_{\mathbf{ik}}} \tag{6}$$

From Eq. (6), it is clear that the sensitivity of the one-pin ABC frequencies to a particular structural parameter is a combination of the respective sensitivity of mode shapes at the same point and the sensitivity of the natural frequencies.

Hanson et al. [29] also proposed the expression of anti-resonance sensitivity. A two-DOF system was used in their study, leading to a simplified expression of the FRF from Eq. (2) with n=2, and the subsequent sensitivity of the anti-resonance is effectively a special case of Eq. (6).

Theoretically speaking, based on Eq. (6), it is possible to calculate the contributions ("footprint") of the mode shapes in the driving-point anti-resonance (one-pin ABC)

frequency sensitivities. Hanson et al. [29] employed a ratio to represent the mode shape contributions in the sensitivities of the anti-resonances, with the following expression:

$$C = \frac{|\Phi|}{|\Omega| + |\Phi|} \tag{7}$$

where C is the relative mode shape contribution ratio, Ω denotes the natural frequency contribution in the anti-resonance (1-pin ABC) sensitivity, and Φ is the mode shape contribution in the anti-resonance (1-pin ABC) sensitivity,

$$\Omega = \frac{\sum_{p=1}^{m} \frac{\partial \omega_p^2}{\partial p} \left(\sum_{\substack{k=1 \\ k \neq p}}^{m} \det\left(\Lambda - \omega_{i\_pin\_j}^2 I\right)_{k,p} \Phi_{ik} \Phi_{ik} \right)}{\sum_{k=1}^{m} \Phi_{ik} \left(\sum_{\substack{p=1 \\ p \neq k}}^{m} \det\left(\Lambda - \omega_{i\_pin\_j}^2 I\right)_{k,p} \right) \Phi_{ik}} \tag{7a}$$

$$\Phi = 2 \times \frac{\sum_{k=f}^{m} \frac{\partial \Phi_{ik}}{\partial p} \det\left(\Lambda - \omega_{i\_pin\_j}^2 I\right)_{k} \Phi_{ik}}{\sum_{k=f}^{m} \Phi_{ik} \left(\sum_{\substack{p=1 \\ p \neq k}}^{m} \det\left(\Lambda - \omega_{i\_pin\_j}^2 I\right)_{k,p} \right) \Phi_{ik}} \tag{7b}$$

The effectiveness of using the ratio in a two-DOF system has been verified with both numerical and experimental studies [29]. Thus, the (1-pin) ABC frequencies that contain a larger mode shape contribution are expected to be relatively more sensitive to damage and hence should be selected for the FE model updating.

2.2 Two-pin ABC frequency sensitivity and mode shape contributions

The above method of evaluating the anti-resonance (1-pin ABC) frequency sensitivity can be extended to two-pin ABC frequencies, thus Eq. (7) can also be employed to obtain mode shape contributions in the two-pin ABC frequency sensitivities.

As described in previous studies [20-21], two-pin ABC frequencies can be obtained by inverting the 2×2 FRF matrix measured at these two pin points, and each element (ABC curve) in the inverted matrix can be used to determine the two-pin ABC frequencies by identifying the singular (peak) frequencies.

For simplicity, consider only the first three natural modes in the structural response, the 2×2 FRF matrix can then be expressed as:

$$\mathbf{H} = \begin{bmatrix} \mathbf{h}_{ii} & \mathbf{h}_{ij} \\ \mathbf{h}_{ji} & \mathbf{h}_{jj} \end{bmatrix} \tag{8}$$

where h_{ii} is the FRF containing the first three modes of information,

$$\mathbf{h}_{ii} = \frac{\omega_{i1}^2}{\omega_1^2-\omega^2} + \frac{\omega_{i2}^2}{\omega_2^2-\omega^2} + \frac{\omega_{i3}^2}{\omega_3^2-\omega^2} \tag{8a}$$

Inverting the above matrix yields:

$$\mathbf{H}^{-1} = \frac{1}{\left|\mathbf{h}_{ii}\mathbf{h}_{jj} - \mathbf{h}_{ij}\mathbf{h}_{ji}\right|}\begin{bmatrix} \mathbf{h}_{jj} & -\mathbf{h}_{ij} \\ -\mathbf{h}_{ji} & \mathbf{h}_{ii} \end{bmatrix}$$

(9)

From Eq. (9), the singular (peak) frequencies in the inverted matrix, i.e. the two-pin ABC frequencies, can be calculated by setting $\left|h_{ii}h_{jj} - h_{ij}h_{ji}\right|$ to zero:

$$\left(\frac{\varphi_{i1}^2}{\omega_1^2-\omega_{2-pin}^2} + \frac{\varphi_{i2}^2}{\omega_2^2-\omega_{2-pin}^2} + \frac{\varphi_{i3}^2}{\omega_3^2-\omega_{2-pin}^2}\right)\left(\frac{\varphi_{j1}^2}{\omega_1^2-\omega_{2-pin}^2} + \frac{\varphi_{j2}^2}{\omega_2^2-\omega_{2-pin}^2} + \frac{\varphi_{j3}^2}{\omega_3^2-\omega_{2-pin}^2}\right) - \left(\frac{\varphi_{i1}\varphi_{j1}}{\omega_1^2-\omega_{2-pin}^2} + \frac{\varphi_{i2}\varphi_{j2}}{\omega_2^2-\omega_{2-pin}^2} + \frac{\varphi_{i3}\varphi_{j3}}{\omega_3^2-\omega_{2-pin}^2}\right)^2 = 0 \tag{10}$$

From Eq. (10), the two-pin ABC frequencies with pins at i and j can be represented as:

$$\omega_{2-pin}^2 = \frac{A1\times\omega_3^2 + A2\times\omega_2^2 + A3\times\omega_1^2}{A1 + A2 + A3} \tag{11}$$

where $A1 = \left(\varphi_{i1}\varphi_{j2} - \varphi_{i2}\varphi_{j1}\right)^2$, $A2 = \left(\varphi_{i1}\varphi_{j3} - \varphi_{i3}\varphi_{j1}\right)^2$, $A3 = \left(\varphi_{i2}\varphi_{j3} - \varphi_{i3}\varphi_{j2}\right)^2$

The derivative of two-pin ABC frequencies with respect to a variable parameter p can be further expressed as follows:

$$\frac{\partial\omega_{2-pin}^2}{\partial p} = \frac{\left(\frac{\partial A1}{\partial p}\omega_3^2 + \frac{\partial\omega_3^2}{\partial p}A1 + \frac{\partial A2}{\partial p}\omega_2^2 + \frac{\partial\omega_2^2}{\partial p}A2 + \frac{\partial A3}{\partial p}\omega_1^2 + \frac{\partial\omega_1^2}{\partial p}A3\right)(A1 + A2 + A3)}{(A1 + A2 + A3)^2} - \frac{\left(\frac{\partial A1}{\partial p} + \frac{\partial A2}{\partial p} + \frac{\partial A3}{\partial p}\right)\left(A1\times\omega_3^2 + A2\times\omega_2^2 + A3\times\omega_1^2\right)}{(A1 + A2 + A3)^2} \tag{12}$$

where $\frac{\partial A1}{\partial p} = 2\left(\varphi_{i1}\varphi_{j2} - \varphi_{i2}\varphi_{j1}\right)\left(\frac{\partial\varphi_{i1}}{\partial p}\varphi_{j2} + \varphi_{i1}\frac{\partial\varphi_{j2}}{\partial p} - \frac{\partial\varphi_{i2}}{\partial p}\varphi_{j1} - \varphi_{i2}\frac{\partial\varphi_{j1}}{\partial p}\right)$

$$\frac{\partial A2}{\partial p} = 2\left(\varphi_{i1}\varphi_{j3} - \varphi_{i3}\varphi_{j1}\right)\left(\frac{\partial\varphi_{i1}}{\partial p}\varphi_{j3} + \varphi_{i1}\frac{\partial\varphi_{j3}}{\partial p} - \frac{\partial\varphi_{i3}}{\partial p}\varphi_{j1} - \varphi_{i3}\frac{\partial\varphi_{j1}}{\partial p}\right) \tag{13}$$

$$\frac{\partial A3}{\partial p} = 2\left(\varphi_{i2}\varphi_{j3} - \varphi_{i3}\varphi_{j2}\right)\left(\frac{\partial\varphi_{i2}}{\partial p}\varphi_{j3} + \varphi_{i2}\frac{\partial\varphi_{j3}}{\partial p} - \frac{\partial\varphi_{i3}}{\partial p}\varphi_{j2} - \varphi_{i3}\frac{\partial\varphi_{j2}}{\partial p}\right)$$

According to Eq. (12) and (13), it can be observed clearly that similar to one-pin ABC frequency sensitivity, the sensitivity of two-pin ABC frequency can also be expressed with a

combination of the natural mode shape sensitivities at the same points and the natural frequency sensitivities.

The mode shape contribution in the two-pin ABC frequency sensitivities can also be evaluated using Eq. (7), but the values of the mode shape sensitivity and natural frequency sensitivity are now expressed as:

$$\Phi = \frac{\left(\frac{\delta A1}{\delta p}\omega_1^2 + \frac{\delta A2}{\delta p}\omega_2^2 + + \frac{\delta A3}{\delta p}\omega_3^2 + \right)(A1 + A2 + A3)}{(A1 + A2 + A3)^2} - \frac{\left(\frac{\delta A1}{\delta p} + \frac{\delta A2}{\delta p} + \frac{\delta A3}{\delta p}\right)(A1 \times \omega_1^2 + A2 \times \omega_2^2 + A3 \times \omega_3^2)}{(A1 + A2 + A3)^2}$$

$$\Omega = \frac{\left(\frac{\partial \omega_3^2}{\partial p} A1 + \frac{\partial \omega_2^2}{\partial p} A2 + \frac{\partial \omega_1^2}{\partial p} A3\right)(A1 + A2 + A3)}{(A1 + A2 + A3)^2} \quad (14)$$

In what follows, a numerical case is employed to illustrate the outcome and the soundness of the one-pin and two-pin ABC frequency sensitivities with the above equations, before utilizing them in the process of selecting ABC frequencies for FE model updating.

3. Numerical verification of ABC frequency sensitivities

A beam model is used for the numerical verification. Both one-pin and two-pin ABC frequency sensitivities are calculated using equations in Section 2, and these results are compared with those from the direct method, where the ABC frequency sensitivity is calculated using the ABC frequencies of the beam before and after the damage.

The beam is tested and simulated to validate ABC frequency sensitivities from above equations. It is 1m long, and the cross section is 50 × 6 mm, and is made of steel. The beam is fully fixed at both ends. The rigidity (EI) of the beam model is slightly tuned from the theoretical value to 162 $N.m^2$ so that its natural frequencies match those from the test beam with the same dimension and boundary condition, allowing for easy comparisons in other aspects where needed, for example, the one-pin and two-pin ABC frequencies are extracted from the test beam and compared to those from the model to verify the accuracy of the experimental extracted ABC frequencies, which is beyond the scope of this paper.

The first three natural frequencies from the FE model beam are 29.6Hz, 81.6Hz and 160Hz, respectively. The beam is divided into ten elements, thus nine measurement points can be employed to obtain ABC frequencies, as depicted in Fig. 1.

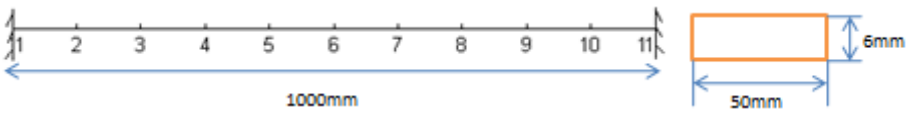

Figure 1 FE model of beam

For convenience, only the first order ABC frequencies are employed in the verification here. Similar observations can be extended to higher (2nd and 3rd) ABC frequencies as well.

A damage scenario is simulated with a 1% stiffness reduction at element 3, which is shown in Fig. 2.

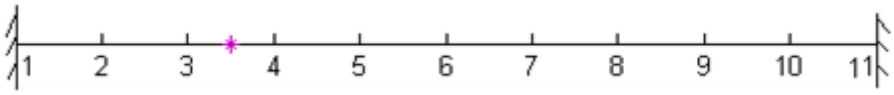

Figure 2 An arbitrary damage scenario in the beam

One-pin ABC frequency sensitivity is examined firstly. Given the beam properties, the sensitivity of one-pin ABC frequencies can be obtained using Eq. (6). It is noted that in the present calculation only the first three natural modes are used to form the FRF data.

Fig.3 compares the results using the sensitivity equations with those calculated directly from the ABC frequencies before and after damage (direct method). The vertical axis is the sensitivity of squared one-pin ABC frequency, which is shown in Eq. (6).

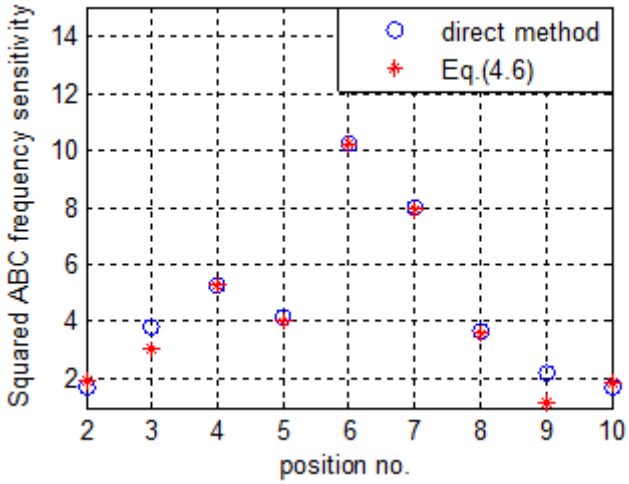

Figure 3 One-pin ABC frequency sensitivities (to damage in segment 3) obtained using different methods

It can be seen that the one-pin ABC frequency sensitivities calculated using Eq. (6) compare well with the direct results. The slight difference may be attributed to the fact that only the first few modes are employed to calculate the one-pin ABC frequency sensitivity using the equations. The variation of the sensitivity indicates that the one-pin ABC frequency (first order herein) shows the highest sensitivity when the pin is positioned at point 6, i.e. the mid-span. This is explicable as the first order ABC frequency when the pin is in the middle has the highest curvature over segment 3 where the particular damage is located.

Next, the sensitivity of two-pin ABC frequencies is examined. The two-pin ABC frequency sensitivities calculated using Eq. (12) and (13) are compared with the direct results of the two-pin ABC frequencies before and after damage. Fig. 4 shows the comparison. Note that numbers in the x-label indicates the two pin positions, for example, “12” means pins located at points 1 and 2. The vertical axis is the sensitivity of squared two-pin ABC frequency shown in Eq. (12). It should be noted that although sensitivities of various two-pin ABC frequencies, including two-pin ABC frequencies with closely located pins and well separated pins, are compared, only sensitivities of adjacent two-pin ABC frequencies are shown in Fig. 4 to cover all the pin locations.

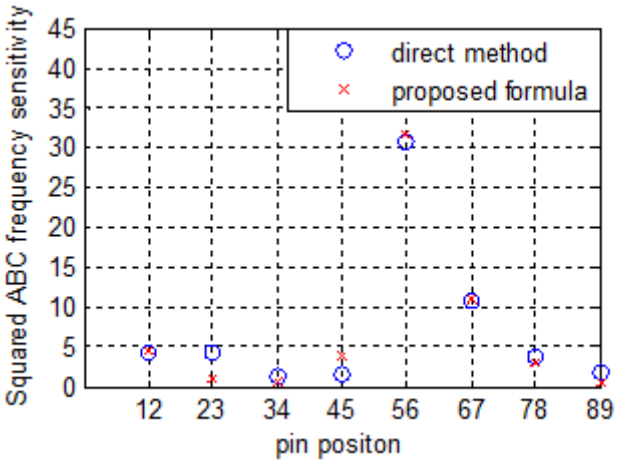

Figure 4 Two-pin ABC frequency sensitivities using different methods

It can be observed that the sensitivities evaluated using Eq. (12) and (13) agree well with the direct results. Similar to comparison results of one-pin ABC frequency sensitivity, the difference may be attributed to the fact that only the first few modes are used in the calculation with Eq. (12) and (13).

The above comparisons confirm that both one-pin and two-pin ABC frequency sensitivities can be satisfactorily evaluated using equations described in Section 2, which also indicates that these sensitivities are closely correlated with the first few (three herein) natural modes. This paves a way for the proposal of a methodology to select the ABC frequencies to be measured / included in a particular damage identification procedure.

4. Selection of optimal ABC frequencies for structural damage identification and numerical validation

4.1 Selection methodology

The sensitivity of an ABC frequency is defined with respect to a particular structural parameter, as expressed in Eq. (6), (12) and (13). For a set of different structural parameters, a set (vector) of ABC frequency sensitivities can be obtained. Therefore, depending upon whether or not prior knowledge about the damage positions is available, the selection method will differ.

4.1.1 Selection of ABC frequencies with prior knowledge of damage positions

When prior knowledge about the damage (stiffness reduction in particular) positions is available, the selection process is straightforward. The sensitivity of one-pin and two-pin ABC frequencies with respect to the stiffness of the damaged element can be calculated using Eq. (6), (12) and (13), then the mode shape contributions in the corresponding ABC frequency sensitivities can be obtained using Eq. (7). The ABC frequencies which exhibit higher mode shape contributions are selected, subject to a desirable total number, for FE model updating.

4.1.2 Selection of ABC frequencies without prior knowledge of damage positions

When the damage positions are not known beforehand, as in most practical applications, the selection needs to be based on the overall sensitivity of the ABC frequency with respect to all possible damage positions.

Generally speaking, assuming a structure with n elements, for a particular ABC frequency, its sensitivity to a damage (stiffness reduction) in element i is defined as S_i, thus in total n sensitivities of the ABC frequency can be obtained, the sensitivity vector **S** containing these sensitivities can be written as (S_1, S_2, …, S_{n-1}, S_n). For each ABC frequency sensitivity, the mode shape contribution index C can be calculated using Eq. (7), thus a vector of index **C** can be formed as **C** = (C_1, C_2, …, C_{n-1}, C_n). Based on the mode shape contribution vector **C**, the overall sensitivity of an ABC frequency may be expressed as:

$$\overline{C} = \mu_C + \mu_C / \sigma_C \tag{15}$$

where μ_C and σ_C are mean value and standard deviation of the vector **C**.

With the above index $\overline{C}$, the ABC frequencies with higher mean value and smaller standard deviation value will be selected, which means these ABC frequency sensitivities have collectively higher mode shape contributions to all possible damage scenarios.

Take the beam with ten elements shown in Fig. 1 as an example. There could be ten possible single damage positions. For each ABC frequency, a sensitivity vector **S** includes ten sensitivities with respect to elemental stiffness of ten possible positions, which can give ten mode shape contributions in vector **C**. Subsequently the $\overline{C}$ value in Eq. (15) can be calculated for the selection of ABC frequencies.

Fig. 5 depicts the index values of different ABC frequencies from the above beam, these frequencies include the first two orders of one-pin ABC frequencies and the first order two-pin ABC frequencies. From the figure it can be seen that the proposed index values stretch over a diverse range, from 20 to 60 herein, and this indicates that separation (selection) of the more sensitive ABC frequencies can be made using the index without ambiguity.

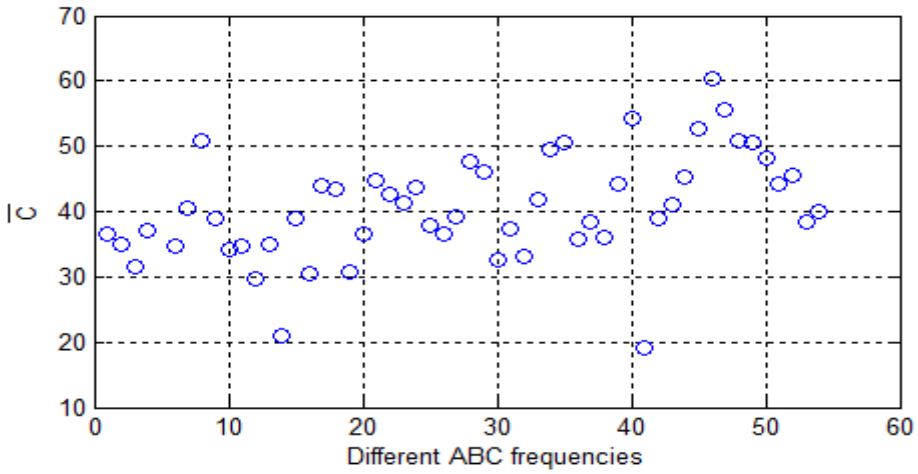

Figure 5 ABC frequency sensitivity index (mode shape contribution ratio) values

4.2 Numerical verification of the selection criteria

4.2.1 Numerical validation with prior knowledge of damage positions

The same beam model mentioned above (shown in Fig. 1) is used to verify the performance of the selection method in FE model updating.

For first scenario with prior knowledge of the damage position, an arbitrary single damage is simulated by a 50% stiffness reduction at the 3rd element. The candidate ABC frequencies include the first two orders of one-pin ABC frequencies and the first order two-pin ABC frequencies. For comparison, two different sets of ABC frequencies are used for FE model updating. The first set includes ten ABC frequencies having larger mode shape contributions, while the second set includes ten ABC frequencies having smaller mode shape contributions. It should be mentioned that for the present verification, the ABC frequencies are free of noises (no noises added), and thus the difference in the updating results is only attributable to the performance of the selected ABC frequencies.

The actual structural damage identification is carried using a genetic-algorithm (GA) powered identification procedure. According to previous studies about GA application [26], in most cases, the probabilities for crossover and mutation can be selected within 0.6-0.9 and 0.01-0.02 to achieve reasonable solutions, but a lower crossover probability and higher mutation probability should be used for real coding GA. Therefore, in this study, the probabilities for crossover and mutation are selected as 0.7 and 0.02, respectively. These parameters are listed in the Table 1.

Table 1 GA configuration

Max generation	1,000
Selection method	Ranking selection
Crossover method	Heuristic crossover
Crossover probability	0.7
Mutation method	Uniform mutation
Mutation probability	0.02

Fig. 6 depicts the updating results using the two different sets of ABC frequencies datasets, the corresponding root mean square errors and the maximum percentage errors in the updating results. It is noted that the parameters being updated are represented by a stiffness ratio, which is defined as the ratio between the variable elemental rigidity and the original (undamaged) elemental rigidity.

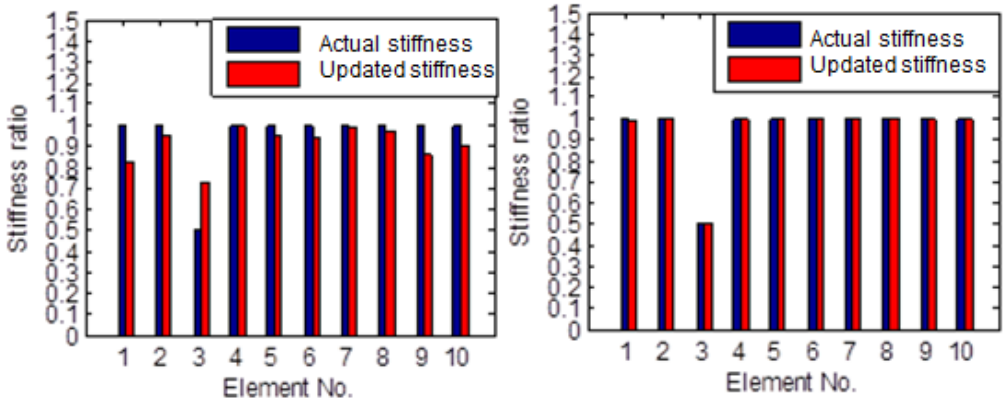

Using 10 "worst ABC frequencies **Using 10 "best" ABC frequencies**

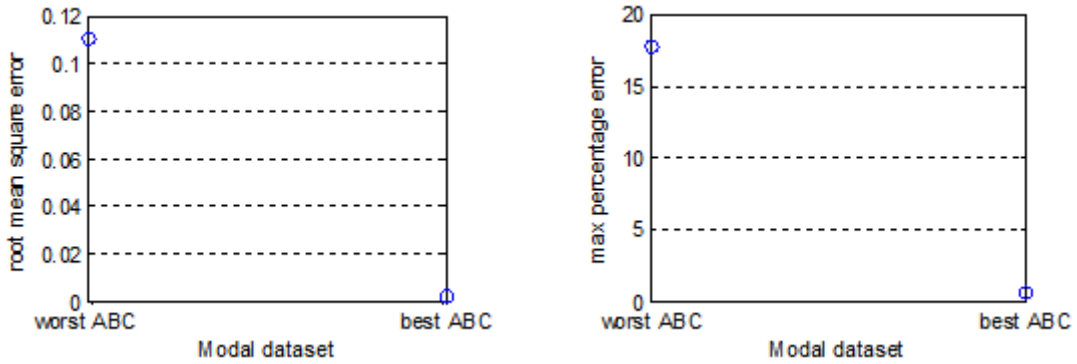

Root mean square error **Max percentage error**

Figure 6 Updating results using different ABC frequencies (noise-free) and comparison

From the updating results shown in Fig. 6, it can be seen that the performance of the "best" 10 ABC frequencies selected by the mode shape contribution criterion is superior over that of the 10 "worst" ABC frequencies. Without the influence of measurement noises, the accuracy of the updating results using the 10 "best" ABC frequencies is almost perfect, with a root mean square error (RMSE) and maximum percentage error (MPE) approaching zero. On the other hand, with the "worst" 10 ABC frequencies, the RMSE and MPE of the updated results are about 11% and 18%, respectively.

To further evaluate the effect of the selection method under practical conditions, the computed (exact) ABC frequencies are treated by injecting measurement noises before they are employed in the FE updating procedure. For this purpose, a 1% uniformly distributed random error is added to the ABC frequencies to simulate more realistic ABC frequencies as would be extracted from an experiment. Fig. 7 shows the FE model updating results using noise-contaminated ABC frequencies. For comparison, results using 4 sets of ABC frequencies, ranging from collectively the "worst" to the "best" sets according to the different ABC frequency sensitivity index ($\overline{C}$) values calculated using Eq. (15), are presented. It should be mentioned that the same number (ten) ABC frequencies is used in each set.

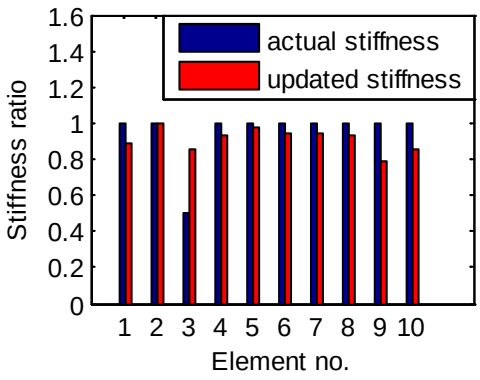

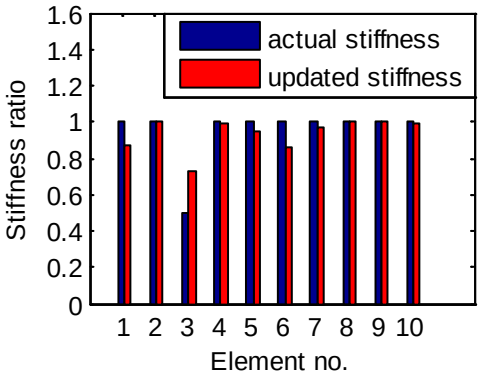

313

314 $\overline{C}$ < 35 35< $\overline{C}$ <40

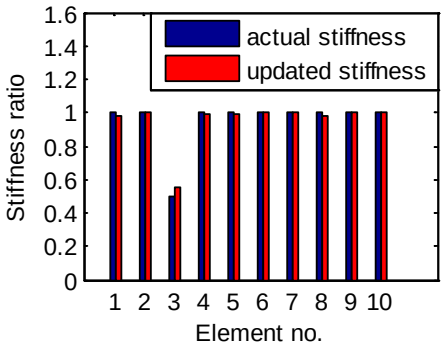

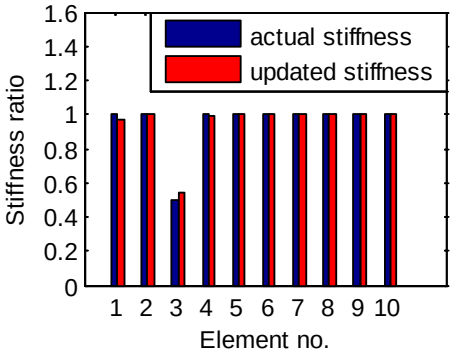

315

316 40< $\overline{C}$ <47 $\overline{C}$ >47

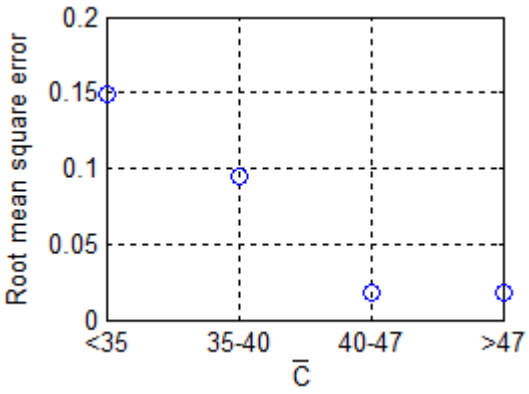

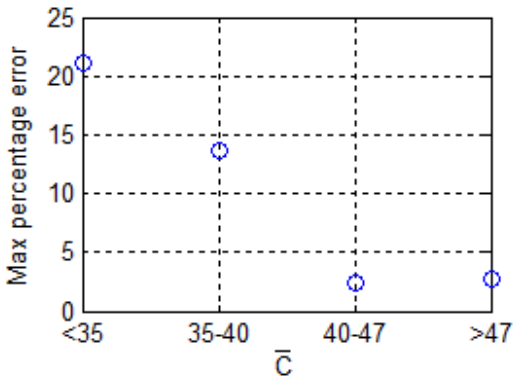

317

318 **Root Mean Square Error** **Max percentage error**

319 **Figure 7 Updating results using different ABC frequencies (noise added) and comparison**

320 The results and comparison further confirm that, even with the inclusion of the
321 measurement noises in the ABC frequencies, the employment of "better" ABC frequencies
322 that contain higher mode shape contributions tends to yield better updating results. When
323 the "worst" set of ABC frequencies with ABC frequency sensitivity value $\overline{C}$ less than 35 is
324 used, the updated results exhibit errors as large as 15% in terms of RMSE and 25% in terms
325 of MPE. On the other hand, when the "best" set of ABC frequencies is used, the updating
326 results are very good with only about 2% RMSE and 3% MPE.

327 4.2.2 Numerical validation without prior knowledge of damage positions

For this verification, different damage scenarios are considered to examine the performance of the proposed index in Eq. (15). Similar to the analysis in the above section, two datasets of ABC frequencies are employed in the FE model updating procedure. The first dataset includes ten ABC frequencies having the largest sensitivity index values (in terms of the mode shape contributions), while ten ABC frequencies with the smallest index values are used in the second dataset. 1% uniformly distributed random noises are added to the ABC frequencies to simulate measurement errors in all the ABC frequencies. The updating results are illustrated in Fig. 8.

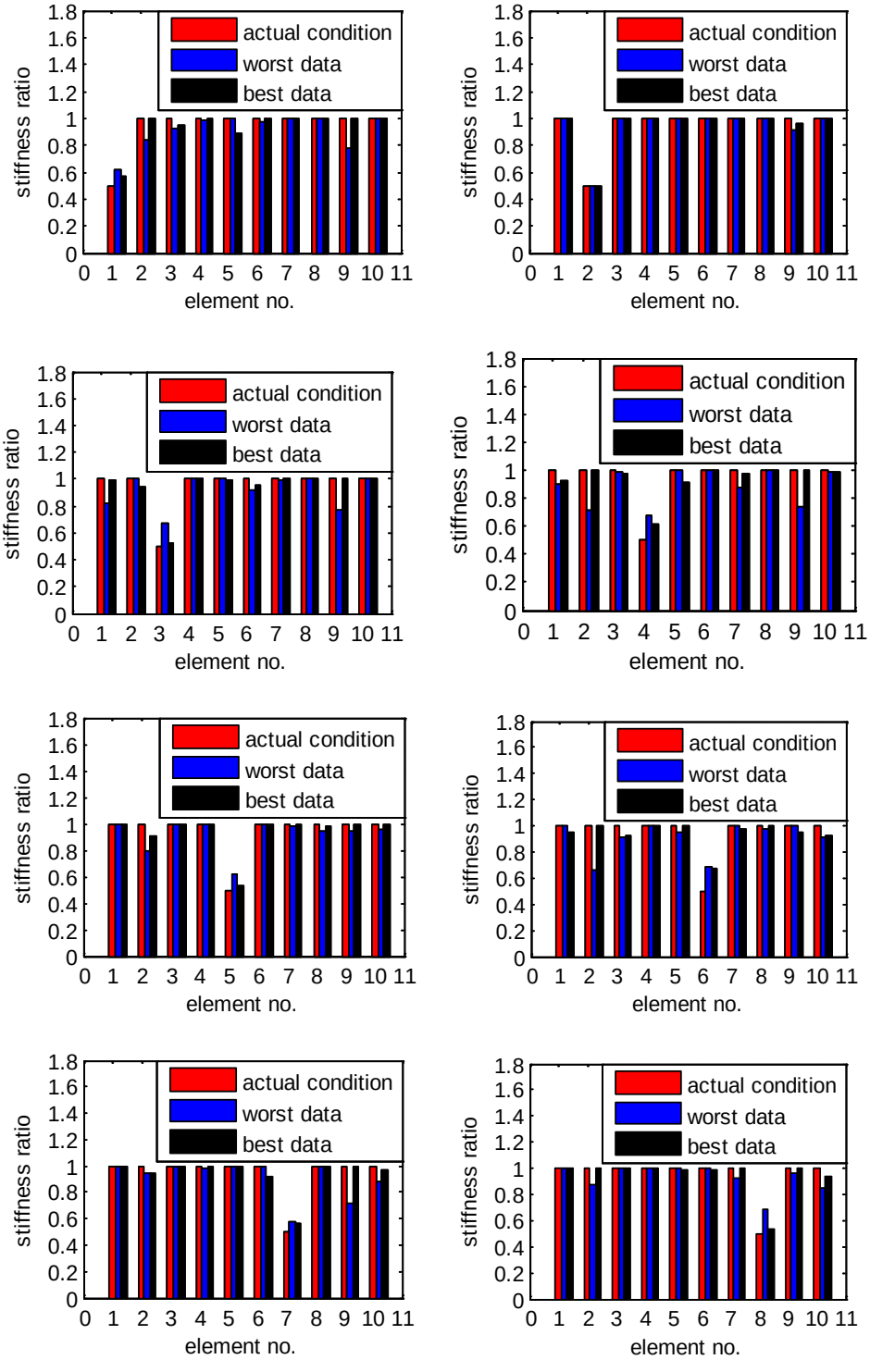

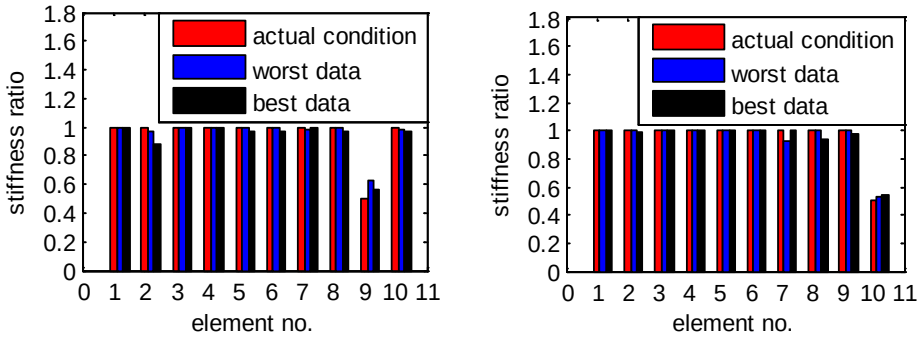

(a) Updating results for damage in element 1 to 10 consecutively

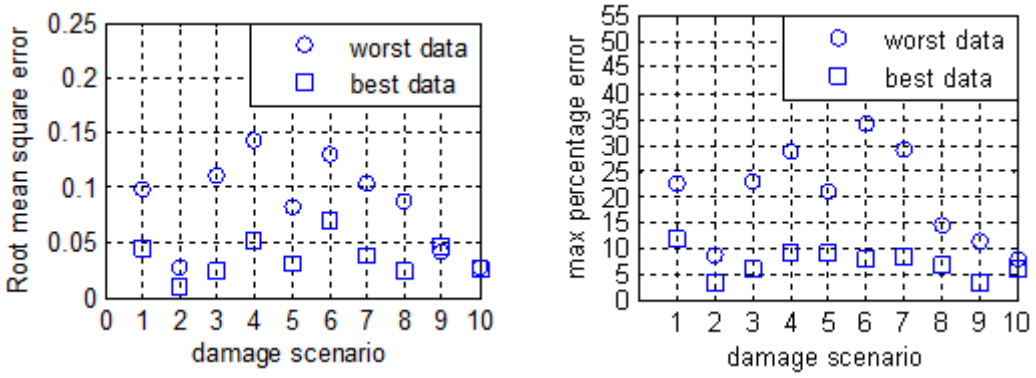

(b) Updating errors (RMSE and MPE) for each damage scenario

Figure 8 Updating results using the "best" and "worst" sets of ABC frequencies for various damage scenarios

From the results shown in Fig. 8, it can be seen that the performance of the "best" ten ABC frequencies is clearly and consistently superior over the "worst" ten ABC frequencies. Using the ten "best" ABC frequencies, the maximum RMSE and MPE of updated results are about 7% and 12%, respectively; whereas with the "worst" ten ABC frequencies the maximum RMSE and MPE in the updating results can approach as high as 15% and 35%, respectively.

It is worth noting that there exists differences in the updating results for the symmetrical damage scenarios, while theoretical speaking, the updating results for symmetrical cases should be exactly the same. These differences can be attributed to two factors; one is that the added 1% noise in the frequencies may cause variation in the updating results, and another is that the searching path in GA may not be the same in each case, which will also give different updating results.

It should be pointed out that in all the above numerical simulations, only a single damaged element has been assumed in each individual case. This is mainly for the convenience of presenting and comparing the results across different damage scenarios. In fact, during the model updating, all elements have been assumed to have variable damage (stiffness) parameters. Therefore, as far as the model updating procedure is concerned, the observations are generally applicable, regardless whether the problem involves just one or multiple damage locations. For illustration, two multiple-damage cases are considered and the updating is performed also using the 'best' and 'worst' ten ABC frequencies, respectively. The results are shown in Fig. 9. It can be observed that for multiple damage scenarios, the 'best' ten ABC frequencies still perform better than the 'worst' ten ABC frequencies.

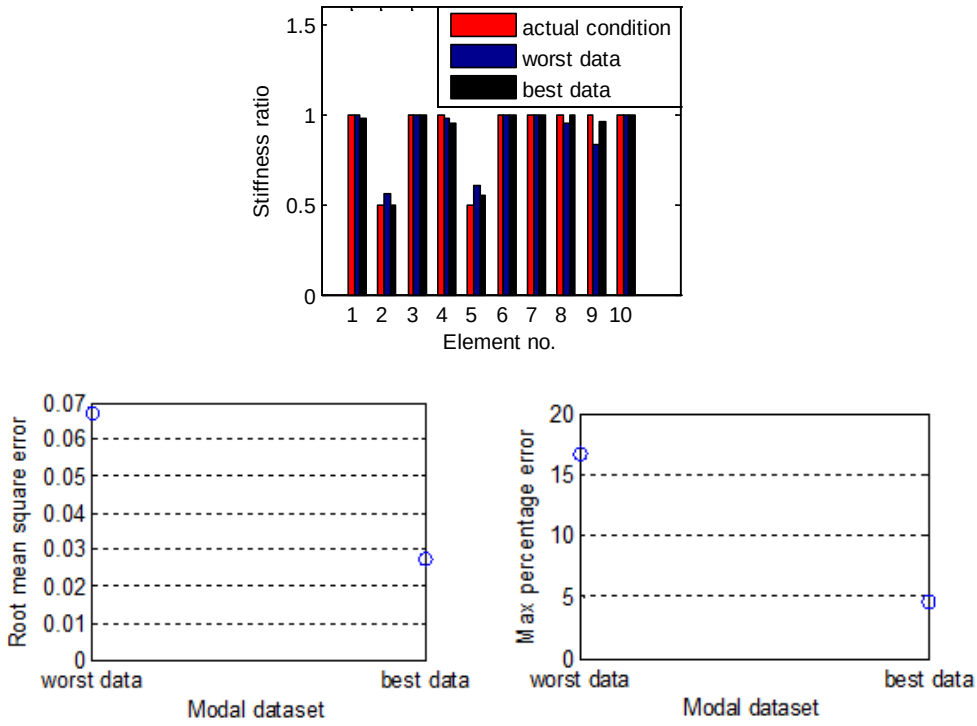

(a) 50% stiffness reductions at elements 2 and 5

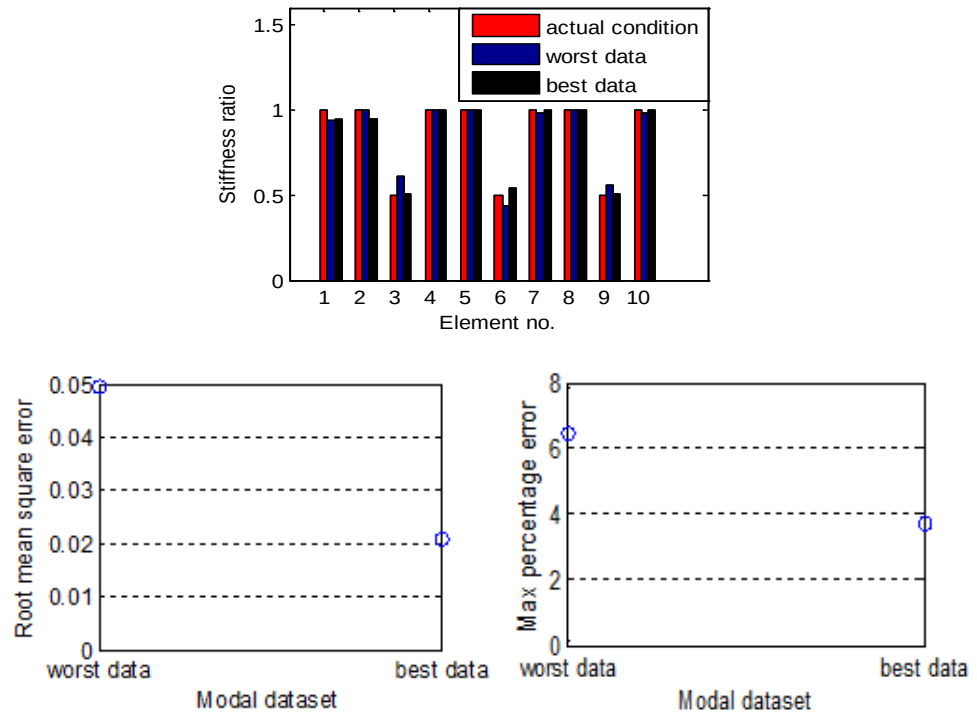

50% stiffness reductions at elements 3, 6 and 9

Figure 9 Updating results using the "best" and "worst" sets of ABC frequencies for multiple damage scenarios

It should be pointed out that in the above numerical examples, ten unknown parameters are updated using only ten ABC frequencies, which is deemed adequate for cross-comparison between the use of different sets of ABC frequencies (with different ranges of the sensitivity

index). A general examination with regard to the effect of the ABC data size on the updating results will be carried out in the next section.

5. Investigation of size of ABC frequency dataset in structural damage identification

As mentioned in previous sections, there is an optimum range of the amount of modal data to be included in a FE model updating procedure. It is generally understood that the number of modal data should be 2-3 times the number of parameters being updated in order to achieve a satisfactory result [30]. Due to inevitable measurement errors, employing too many modal data could introduce conflicting tendencies during the updating process and thus adversely affect the updating results, and evidences of such phenomenon have been reported in a number of occasions [31-32]. The use of the rule of "2-3 times" has been adopted in many previous studies [25, 31, 33].

In this section, we shall examine whether the above general observations also apply in the case of using ABC frequencies. Firstly, two groups of twenty ABC frequencies are employed for the model updating; one group includes ABC frequencies with larger sensitivity index ($\overline{C}$) values, and the other includes ABC frequencies having smaller sensitivity index values. Thus, the two groups are effectively the expanded sets from the cases using 10 ABC frequencies in Section 4. The updating results and their percentage errors are shown in Fig. 10.

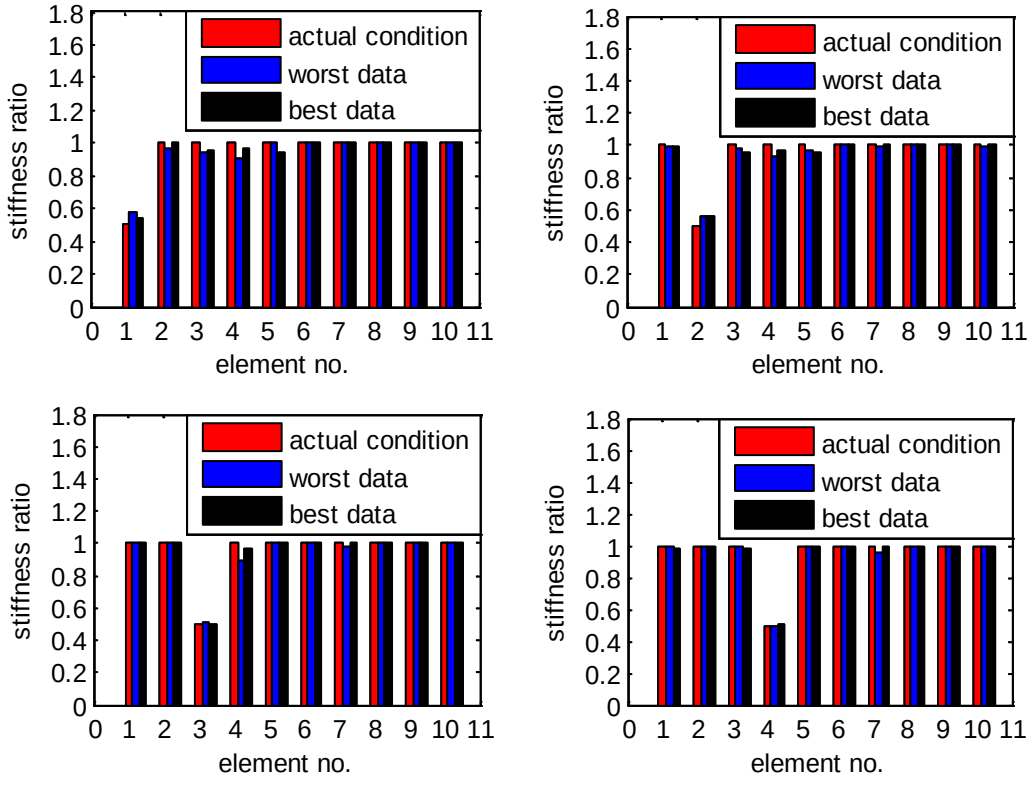

397

398

399

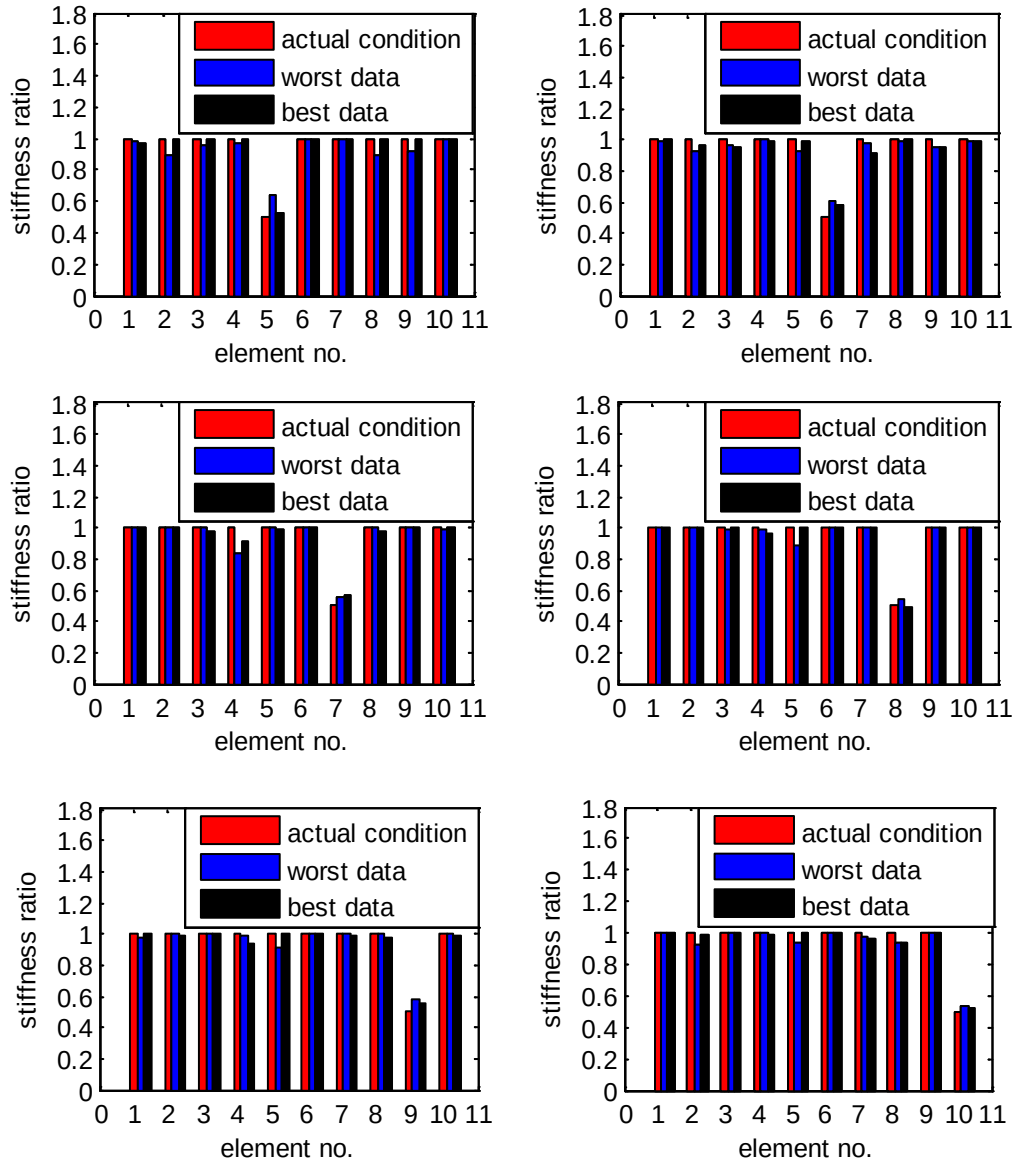

400 **(a) Updating results for damage in element 1 to 10 consecutively**

401

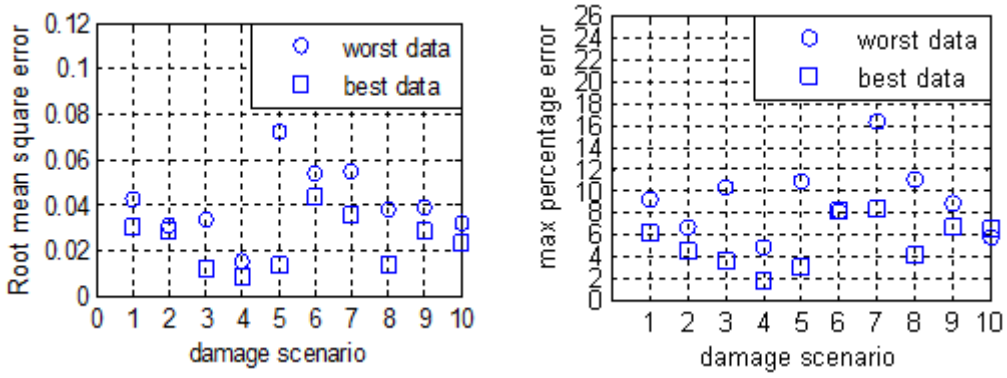

402 **(b) Updating errors (RMSE and MPE) for each damage scenario**

403 **Figure 10 Updating results using 20 ABC frequencies for various damage scenarios**

404 It can be seen that, when 20 ABC frequencies are employed for the updating of 10
405 parameters, the results from the set of ABC frequencies having higher $\overline{C}$ index values still

produce better results. However, comparing with the results using ten ABC frequencies (Fig. 8(b)), increasing to twenty ABC frequencies does not improve the results much further for the case with the "best" ABC frequencies, indicating that the "best" ABC frequencies as selected according to the ABC sensitivity index (mode shape contributions) indeed contain more significant information. On the other hand, increasing to twenty ABC frequencies in the case of the "worst" ABC frequencies does improve the updating results markedly, and this is expected according the "2-3 times" rule mentioned before. In the particular case with ABC frequencies herein, this may be explained by the fact that, although the ABC frequencies with a smaller index contains less (sensitive) mode shape information, by increasing the number of ABC frequencies, the overall mode shape information gets enhanced.

Next, we shall examine the updating results when too many ABC frequencies are involved. For this purpose all 54 ABC frequencies, including one-pin ABC frequencies from the first two modes and two-pin ABC frequencies from the first mode, are employed in the model updating for each damage scenario. Similar to the previous cases, 1% uniformly distributed random noises are added to ABC frequencies to simulate measurement errors. Fig. 11 shows the results in terms of the RMSE and MPE from using 20 ABC frequencies having larger index values and using all 54 ABC frequencies.

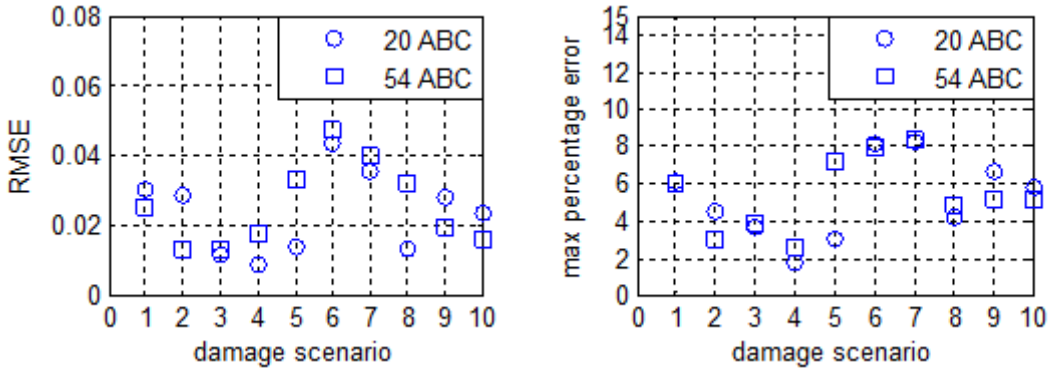

Figure 11 Updating results using different numbers of ABC frequencies

It can be found clearly that by further increasing ABC frequencies for the model updating, results do not show appreciable further improvement. In fact, some results using all 54 ABC frequencies exhibit even larger RMSE and MPE errors than those using 20 ABC frequencies, for example in damage scenarios 4,5,6,7 and 8.

The detailed accuracy profiles will understandably vary as the level of measurement errors (herein assumed 1%) in the ABC frequencies and structural setting vary. However, the results presented above tend to suggest that with ABC frequencies, the general rule on the amount of modal data to be included in the FE model updating still holds. In order words, when employing ABC frequencies in practice (containing some normal level of measurement noises) for model updating, the number of ABC frequencies should be kept about 2-3 times of the number of unknown parameters in order to achieve an effective and efficient FE model updating process.

6. Conclusions

In this paper, the sensitivities of ABC frequencies to damage (stiffness reduction) are studied. On this basis, a methodology for the selection of ABC frequencies in a finite element model updating / damage identification procedure is proposed to achieve the reliable identification results.

For this purpose, the existing anti-resonance (one-pin ABC) frequency sensitivity expression is extended to formulate the two-pin ABC frequency sensitivity expression, which includes the contributions of the natural frequencies and mode shape coordinates at the pin locations. Numerical examples demonstrate that the ABC sensitivity formulas for both one-pin and two-pin ABC frequencies match closely the actual sensitivities as calculated directly from the changes of the respective ABC frequencies corresponding to a particular damage.

The mode shape contribution (ratio) in the ABC frequency sensitivity is adopted as a classifying criterion for the selection of the ABC frequencies in a FE model updating procedure, such that those with higher mode shape contributions are employed, subjected to a desirable number limit.

Numerical studies on the above proposed selection criteria are carried out for different damage scenarios, with or without prior knowledge about damage positions. Results demonstrate that in both situations, the ABC frequencies selected using the proposed criterion consistently give rise to better updating results. Furthermore, it is verified through numerical studies that the general rule regarding the number of modal data to be included in a FE model updating procedure, i.e., being 2-3 times of the number of unknown parameters, also applies in the case with ABC frequencies.

Reference

[1] Vandiver, J.K. (1975). Detection of Structural Failure on Fixed Platforms by Measurement of Dynamic Response. Journal of Petroleum Technology, 305-310.

[2] Begg, R.D., Mackenzie, A.C., Dodds, C.J., Loland, O. (1976). Structural Integrity Monitoring using Digital Processing of Vibration Signals. Proc. 8th Annual Offshore Technology Conference, Houston, TX, 305-311.

[3] Duggan, D.M., Wallace, E.R., Caldwell, S.R. (1980). Measured and Predicted Vibrational Behavior of Gulf of Mexico Platforms. Proc. 12th Annual Offshore Technology, 92-100.

[4] Stubbs, N., Broome, T.H., Osegueda, R. (1990). Monitoring and Evaluating Civil Structures using Measured Vibration. Proc. 14th International Modal Analysis Conference, 84-90.

[5] Stubbs, N., Osegueda, R. (1990). Global Damage Detection in Solids-Experimental Verification. The International Journal of Analytical and Experimental Modal Analysis, 5(2), 81-97.

[6] Hearn, G., Testa, R.B.(1991). Modal Analysis for Damage Detection in Structures. Journal of Structural Engineering, 117(10),3042-3063.

[7] Carrasco, C, et al. (1997). Localization and Quantification of Damage in a Space Truss Model using Modal Strain Energy. Smart Systems for Bridges, Structures and Highways, Proceedings of SPIE, 3043, 181-192.

[8] Doebling, S.W., Farrar, C.R. (1997). Using statistical analysis to enhance modal-based damage identification. Structural damage assessment using advanced signal processing procedures, Proceedings of DAMAS 97, University of Sheffield, UK, 199-210.

[9] Leutenegger, T.(1999). Structural Testing of Fatigued Structures. Smart Structures and Integrated Systems. 3668, 987-997.

[10] Mroz, Z., Lekszynski, T.(2000). Identification of Damage in Structures using Parameter Dependent Modal Response. Proceedings of ISMA25, Noise and Vibration Engineering, Leuven, Belgium.

[11] Koh, B.H., Dyke, S.J. (2007). Structural health monitoring for flexible bridge structures using correlation and sensitivity of modal data. Computers and Structures 85, 117-130.

[12] Gandomi, A.H., Sahab, M.G., Rahaei, A., Safari Gorji, M.(2008). Development in Mode Shape-Based Structural Fault Identification Technique. World Applied Science Journal, 5(1), 29-38.

[13] Gomes, H.G., Silva, N.R.S. (2008). Some comparisons for damage detection on structures using genetic algorithms and modal sensitivity method. Applied Mathematical Modelling, 32, 2216-2232.

[14] Ratcliffe, C.P.(1997). Damage Detection using a Modified Laplacian Operator on Mode Shape Data. Journal of Sound and Vibration, 204(3), 505-517.

[15] Law, S.S., Shi, Z.Y., Zhang, L.M.(1998). Structural Damage Detection from Incomplete and Noisy Modal Test Data. Journal of Engineering Mechanics, 124(11), 1280-1287.

[16] Qiao, P.Z., Lu, K., Lestari, W.Y., Wang, J.L. (2007). Curvature Mode Shape-Based Damage Detection in Composite Laminated Plates. Composite Structures, 80: 409-428.

[17] Doebling, S.W., Farrar, C.R., Prime, M.B., Shevitz, D.W. (1996). Damage Identification and Health Monitoring of Structural and Mechanical Systems from Changes in Their Vibration Characteristics: A Literature Review. Los Alamos National Laboratory.

[18] Sohn, H., Farrar, C.R., Hemez, F.M., Shunk, D.D., Stinemates, D.W., Nadler, B.R., Czarnecki, J.J (2004). A Review of Structural Health Monitoring Literature: 1996-2001. Los Alamos National Laboratory.

[19] Li, S., Shelley, S.J., Brown, D.L.(1995). Perturbed Boundary Condition Testing Concepts. 13th International Modal Analysis Conference (IMAC), Nashville, Tennessee, 13-16.

[20] Gordis, J.H.(1996). Omitted Coordinate Systems and Artificial Constraints in Spatially Incomplete Identification. Modal Analysis, 11, 83-95.

[21] Gordis, J.H.(1999). Artificial Boundary Conditions for Model Updating and Damage Detection. Mechanical Systems and Signal Processing, 13(3), 437-448.

[22] D'Ambrogio, W, Fregolent, A.(2000). The Use of Antiresonances for Robusta Model Updating. Journal of Sound and Vibration, 236(2), 227-243.

[23] Jones K., Turcotte. J.(2002). Finite Element Model Updating using Antiresonant Frequencies. Journal of Sound and Vibration, 252(4): 717-727.

[24] Lu, Y., Mao, L., Tu, Z.G.(2008). Practical Considerations in FE Model Updating with Artificial Boundary Condition Frequencies. The 10th Int. Symposium on Structural Engineering for Young Experts, Changsha, China.

[25] Lu, Y., Tu, Z.G.(2008). Artificial Boundary Condition Approach for Structural Identification: A Laboratory Perspective. Proc., 26th International Modal Analysis Conference, Orlando, Florida.

[26] Tu, Z.G., Lu, Y.(2008). FE Model Updating using Artificial Boundary Conditions with Genetic algorithms. Computers and Structures, 86(7-8), 714-727.

[27] Gordis, J.H., Papagiannakis, K. (2011). Optimal selection of artificial Boundary Conditions for model updating and damage detection. Mechanical Systems and Signal Processing, 25(5), 1451-1468.

[28] Mottershead, J.E.(1998). On the Zeros of Structural Frequency Response Functions and Their Sensitivities. Mechanical Systems and Signal Processing, 12(5), 591-597.

[29] Hanson, D., Waters, T.P., Thompson, D.J., Randall, R.B., Ford, R.A.J.(2007). The Role of Anti-resonance Frequencies from Operational Modal Analysis in Finite Element Model Updating. Mechanical Systems and Signal Processing, 21(1), 74-97.

[30] Kwon, K.S., Lin, R.M. (2003). Frequency selection method for FRF-based model updating. Journal of Sound and Vibration, 278(1-2), 285-306.

[31] Xia, Y., Hao, H. (2000). Measurement selection for vibration-based structural damage identification. Journal of Sound and Vibration, 236(1), 89-104.

[32] He Jimin, Fu Zhifang (2001). Modal analysis. Butterworth-Heinemann, Oxford.

[33] Friswell, M.I., Penny, J.E.T., Garvey, S.D. (1998). A combined genetic and Eigensensitivity algorithm for the location of damage in structures. Computer & Structures, 69(5), 547-556.